

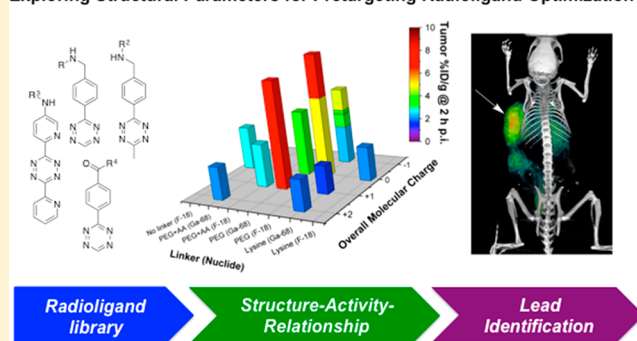
Exploring Structural Parameters for Pretargeting Radioligand Optimization

Jan-Philip Meyer,[†] Paul Kozłowski,[†] James Jackson,[†] Kristen M. Cunanan,[‡] Pierre Adumeau,[§] Thomas R. Dilling,[†] Brian M. Zeglis,^{*,†,§,||,#} and Jason S. Lewis^{*,†,||,#}[†]Department of Radiology, Memorial Sloan Kettering Cancer Center, New York, New York 10065, United States[‡]Department of Epidemiology and Biostatistics, Memorial Sloan Kettering Cancer Center, New York, New York 10065, United States[§]Department of Chemistry, Hunter College of the City University of New York, New York, New York 10065, United States^{||}Ph.D. Program in Chemistry, Graduate Center of the City University of New York, New York, New York 10016, United States[⊥]Program in Molecular Pharmacology, Memorial Sloan Kettering Cancer Center, New York, New York 10065, United States[#]Departments of Radiology and Pharmacology, Weill Cornell Medical College, New York, New York 10065, United States

S Supporting Information

ABSTRACT: Pretargeting offers a way to enhance target specificity while reducing off-target radiation dose to healthy tissue during payload delivery. We recently reported the development of an ¹⁸F-based pretargeting strategy predicated on the inverse electron demand Diels–Alder reaction as well as the use of this approach to visualize pancreatic tumor tissue in vivo as early as 1 h postinjection. Herein, we report a comprehensive structure: pharmacokinetic relationship study of a library of 25 novel radioligands that aims to identify radiotracers with optimal pharmacokinetic and dosimetric properties. This investigation revealed key relationships between molecular structure and in vivo behavior and produced two lead candidates exhibiting rapid tumor targeting with high target-to-background activity concentration ratios at early time points. We believe this knowledge to be of high value for the design and clinical translation of next-generation pretargeting agents for the diagnosis and treatment of disease.

Exploring Structural Parameters for Pretargeting Radioligand Optimization



INTRODUCTION

In vivo pretargeting for diagnostic^{1–6} and therapeutic⁷ applications has emerged over the last three decades as a powerful technology to enhance target specificity and reduce off-target effects.^{2,8} Generally speaking, pretargeting strategies strive to combine the inherent advantages of macromolecular targeting vectors and small molecules, specifically high target specificity and short organ and tissue residence times, respectively.^{1,4} To achieve this, the targeting vector is administered first and allowed to accumulate at the target site and clear from off-target organs prior to the injection of a small effector molecule carrying the payload of interest (e.g., radionuclide; Figure 1).^{4,5,9} To enable their in vivo recombination, both entities are equipped with complementary functionalities that enable an in vivo ligation reaction.^{10,11} Appropriate pairs of reaction partners that have been employed in in vivo pretargeting approaches include streptavidin–biotin,¹² complementary oligonucleotide strands,¹³ and click chemistry-based reaction pairs.^{10,14,15} While strategies based on streptavidin–biotin have shown somewhat deflating outcomes in the clinic,¹⁶ the use of a bispecific, CEA-targeting antibody in combination with a radiolabeled hapten peptide has shown very promising clinical results.¹⁷

One of the newer members of the click chemistry toolbox, the inverse electron-demand Diels–Alder (IEDDA) reaction between *trans*-cyclooctene (TCO) and tetrazine (Tz) has proven particularly well suited for in vivo pretargeting.^{2–5,7,10,11} The IEDDA ligation is selective and bioorthogonal, but its principal advantage for pretargeting compared to other click reactions, such as the Staudinger ligation¹⁸ or the strain-promoted alkyne–azide cycloaddition¹⁴ (SPAAC), lies in its speed. To wit, the first-order rate constants of the Tz/TCO ligation lie in the realm of 10^4 – 10^5 M⁻¹ s⁻¹, orders of magnitude faster than the rates of the Staudinger and SPAAC reactions (0.002 M⁻¹ s⁻¹ and 0.07 M⁻¹ s⁻¹, respectively).¹¹ The in vivo feasibility of the IEDDA reaction between a TCO-modified monoclonal antibody (mAb) and a radiolabeled Tz has been demonstrated by various groups using a wide range of antigen-targeting immunoconjugates and tetrazines labeled with an array of radionuclides for imaging (including ¹¹¹In, ⁶⁴Cu, ^{99m}Tc, ¹⁸F, ⁶⁸Ga, and ¹¹C)^{1,4,5,19–21} and therapy (¹⁷⁷Lu).⁷

Received: August 1, 2017

Published: August 31, 2017

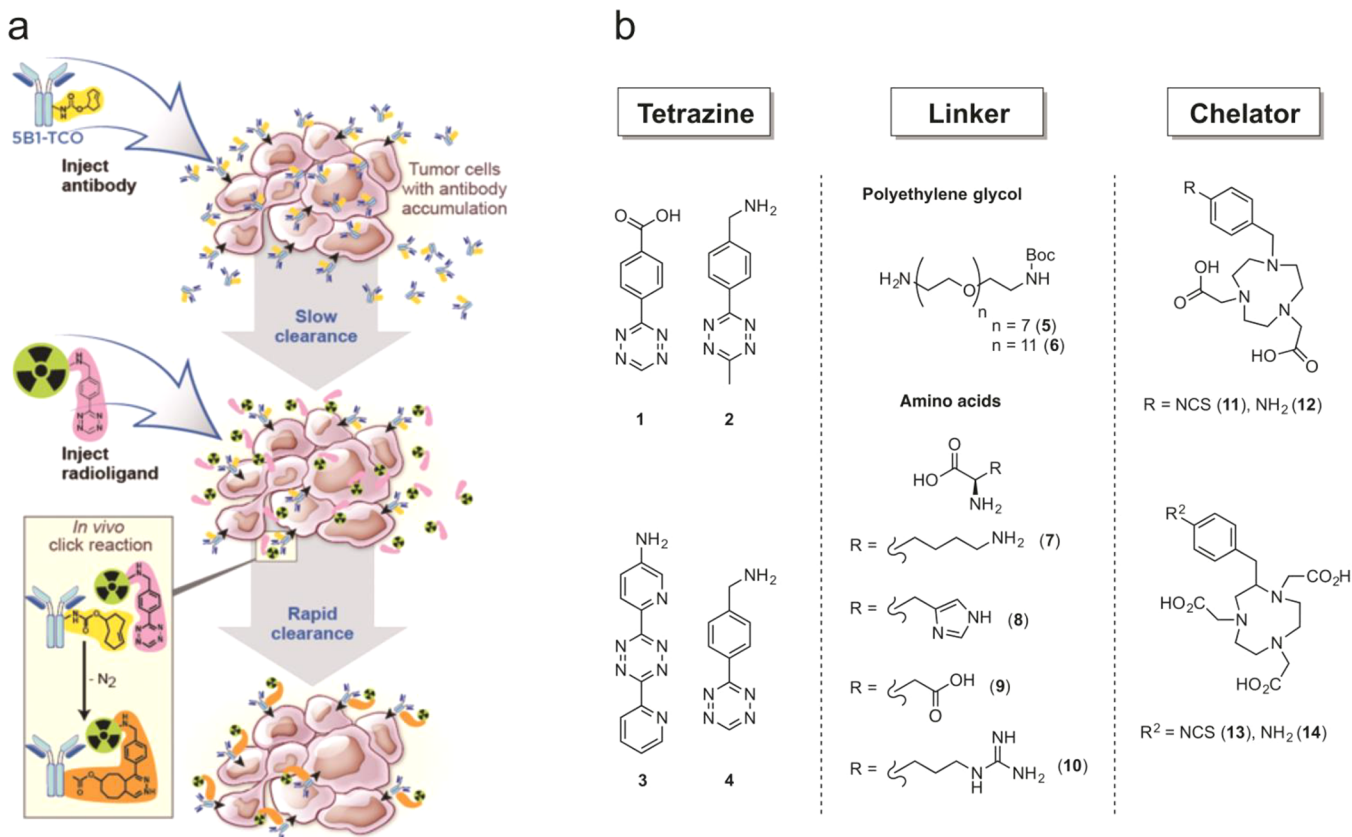


Figure 1. (a) Schematic illustration of the pretargeting approach: a macromolecular targeting vector (in our case an antibody–TCO conjugate) is injected first and allowed to reach the target site while clearing slowly from systemic circulation. After a specific accumulation time, the small molecule effector probe (in this case a radiolabeled tetrazine probe) is administered systemically and undergoes bioorthogonal click reaction with the TCO groups of the immunoconjugate at the target site. (b) Modular chemistry approach for radioligand design: radioligands consisted of a Tz moiety for *in vivo* click chemistry, a linker for altering the biodistribution, and a chelator for the attachment of the positron-emitting metal ions $^{68}\text{Ga}^{3+}$ and ^{18}F -AlF $^{2+}$.

In terms of pretargeted positron emission tomography (PET) imaging, Zeglis et al. presented promising results in 2013 in pretargeting experiments using the gpA33-targeting mAb huA33-TCO and a ^{64}Cu -labeled tetrazine radioligand.⁴ Shortly thereafter, our laboratories developed a second-generation Tz for ^{64}Cu -based pretargeted PET imaging applications by integrating the sarcophagine chelator system into the radioligand structure.³ At the same time, our laboratories demonstrated that an ^{18}F -labeled Tz-based radioligand in combination with the carbohydrate antigen 19.9 (CA19.9)-targeting fully human mAb 5B1-TCO²² allowed for the successful PET imaging of subcutaneous (sc) pancreatic cancer xenografts as early as 1 h postinjection (p.i.).¹ Critically, this new pretargeting approach utilized the short-lived radionuclide ^{18}F ($t_{1/2} = 109$ min), resulting in only a fraction of off-target radiation doses to healthy tissues compared to directly labeled immunoconjugates with long-lived isotopes (^{124}I or ^{89}Zr , $t_{1/2} > 3$ days). Despite clear delineation of tumor tissue at early imaging time points demonstrating the general feasibility of this approach, the relatively low tumor-to-background activity concentration ratios at even 4 h p.i., such as tumor-to-intestines (1.6 ± 0.1) and tumor-to-kidney (1.8 ± 0.4) ratios, inspired us to undertake a thorough investigation into the fundamental relationships between molecular structure, pharmacokinetics, and pretargeting performance.

This first-of-its-kind structure–pharmacokinetics relationship (SPR) study was further fueled by the increased popularity of IEDDA pretargeting strategy. However, current approaches lack fundamental insight into the relationship between physicochemical

properties and pretargeting performance. To address those issues, the study at hand was designed with two main objectives: (1) to identify a radiopharmaceutical lead candidate suitable for clinical development and (2) to generate experimental evidence for a rational understanding of how molecular parameters such as overall molecular net charge, distribution coefficient, plasma half-life (PHL), and stability influence the *in vivo* performance of small-molecule radioligands in pretargeting systems.

Tracer Library and SPR Study Design. The synthesis of the radioligands library as the first step of this study was based on previously reported protocols.^{1,2,4} New reaction routes and radiolabeling procedures developed within this study are described in the Supporting Information (sections 2 and 3). Overall, the radioligands were designed to display structural variation in order to cover a broad spectrum of physicochemical properties, thereby enabling the study of the relationship between structure and *in vivo* behavior (Table 1). Each radioligand is composed of three different structural building blocks (Table 1; Figure 2a). First, a Tz component (1–4) (Scheme 1) was selected for *in vivo* click chemistry. Second, a linker moiety consisting of polyethylene glycol [PEG₇ (5) or PEG₁₁ (6)], amino acids (AA) [AA = lysine (K, 7), histidine (H, 8), aspartate (R, 9), and arginine (D, 10)], or a combination of both is attached. Finally, a bifunctional chelator, either 1,4,7-triazacyclononane-1,4-diacetic acid (NODA, 11,12) or 1,4,7-triazacyclononane-1,4,7-triacetic acid (NOTA, 13,14), was introduced, allowing for the installation of ^{18}F and ^{68}Ga radionuclides. Tz moieties 1–4 were selected based on their previously reported

Table 1. All 25 Radioligands Were Employed in the First Characterization Process^a

Tz	Linker		Chelator	Precursor	Tracer
	PEG _x (x = 7,11)	AA (D, H, K, R)			
1	-	-	NODA	15	[¹⁸ F]15
1	-	K	NOTA	16	[¹⁸ F]16
1	7	-	NOTA	17	[¹⁸ F]17
1	11	-	NOTA	18	[¹⁸ F]18
2	-	K	NOTA	19	[¹⁸ F]19
					[⁶⁸ Ga]19
2	-	K-K	NOTA	20	[¹⁸ F]20
					[⁶⁸ Ga]20
2	-	K-K-K	NOTA	21	[¹⁸ F]21
					[⁶⁸ Ga]21
2	-	K-K-K	NODA	22	[⁶⁸ Ga]22
2	11	-	NOTA	23	[¹⁸ F]23
3	11	-	NOTA	24	[¹⁸ F]24
					[⁶⁸ Ga]24
4	7	-	NODA	25	[¹⁸ F]25
4	7	-	NOTA	26	[⁶⁸ Ga]26
4	11	-	NODA	27	[¹⁸ F]27
					[⁶⁸ Ga]27
4	11	-	NOTA	28	[¹⁸ F]28
					[⁶⁸ Ga]28
4	7	K	NODA	29	[¹⁸ F]29
4	11	H	NODA	30	[¹⁸ F]30
					[⁶⁸ Ga]30
4	11	R	NODA	31	[¹⁸ F]31
4	11	D	NOTA	32	[¹⁸ F]32

^aOn the basis of those results, 15 radioligands were selected for the next step of testing to investigate their performance in pretargeting experiments (blue). Finally, radioligands [¹⁸F]27 and [⁶⁸Ga]27 were identified as lead compounds based on their overall tumoral uptake and tumor-to-NT activity concentration ratios (red).

stability and reaction kinetics with TCO to ensure a wide range of properties.^{4,5,21,23} The use of PEG linkers to modulate in vivo PK of small molecules has previously been reported, including accelerated nontarget organ clearance as well as increased renal clearance.^{1,2,24} We included them into our study in order to investigate their impact on radiotracer PK alone or in combination with AA linkers (which, to the best of our knowledge, have not yet been systematically reported in any SPR study). The amino acids lysine, arginine, histidine, and aspartate were regarded as useful structural components to significantly influence in vivo behavior and PK parameters. It was reasoned that their charged side chains should have a measurable effect on tracer PK and would further allow us to establish a correlation between molecular net charge and PK parameters. Both bifunctional chelator moieties NODA and NOTA currently find broad application in preclinical^{25,26} and clinical²⁷ research for the radiolabeling of biological macromolecules and small molecule targeting probes. Precursors 15–32 were synthesized in good overall chemical yields (18–37%) via 3–8-step syntheses, depending on the starting materials (Figure 2b).

All ¹⁸F- and ⁶⁸Ga-labeled [$t_{1/2}$ (⁶⁸Ga) = 68 min] Tz-derived radioligands were furnished in high radiochemical yields [RCYs.

>55% (¹⁸F); >83% (⁶⁸Ga)], with specific activities (SAs) of >19 MBq/nmol and high radiochemical and radionuclidic purity (Supporting Information, section 3). For in vitro analysis, purified tracers were incubated in human serum at 37 °C to analyze their stability under physiological conditions. Further, the distribution coefficient (log *D*, *n* = 3) of all radioligands in a 1:1 mixture of PBS:1-octanol was determined using the shake-flask method. Subsequently, the tracers (4–8 MBq, 0.5–1 nmol) were injected into healthy athymic nude mice via the lateral tail vein. At various time points (between 2–120 min p.i.), blood was drawn via the lateral tail vein or saphenous vein (*n* = 4) to calculate PHLs (all radioligands, *n* = 1) and plasma stabilities (*n* = 3). Tracers (11–14 MBq, 0.8–1.3 nmol) were injected into healthy athymic nude mice, and general biodistribution experiments for all tracers were performed using serial PET imaging hourly between 1 and 4 h p.i., unless stated otherwise (*n* = 4). Decay-corrected PET imaging data and reconstructed 3D images of the tracer distribution were then used to determine radioactivity concentrations (given as percent injected dose per gram, %ID/g) in the kidney and large intestine (quantitative ROI analysis). Additional ex vivo organ uptake values were determined for selected compounds and were found to be in line with

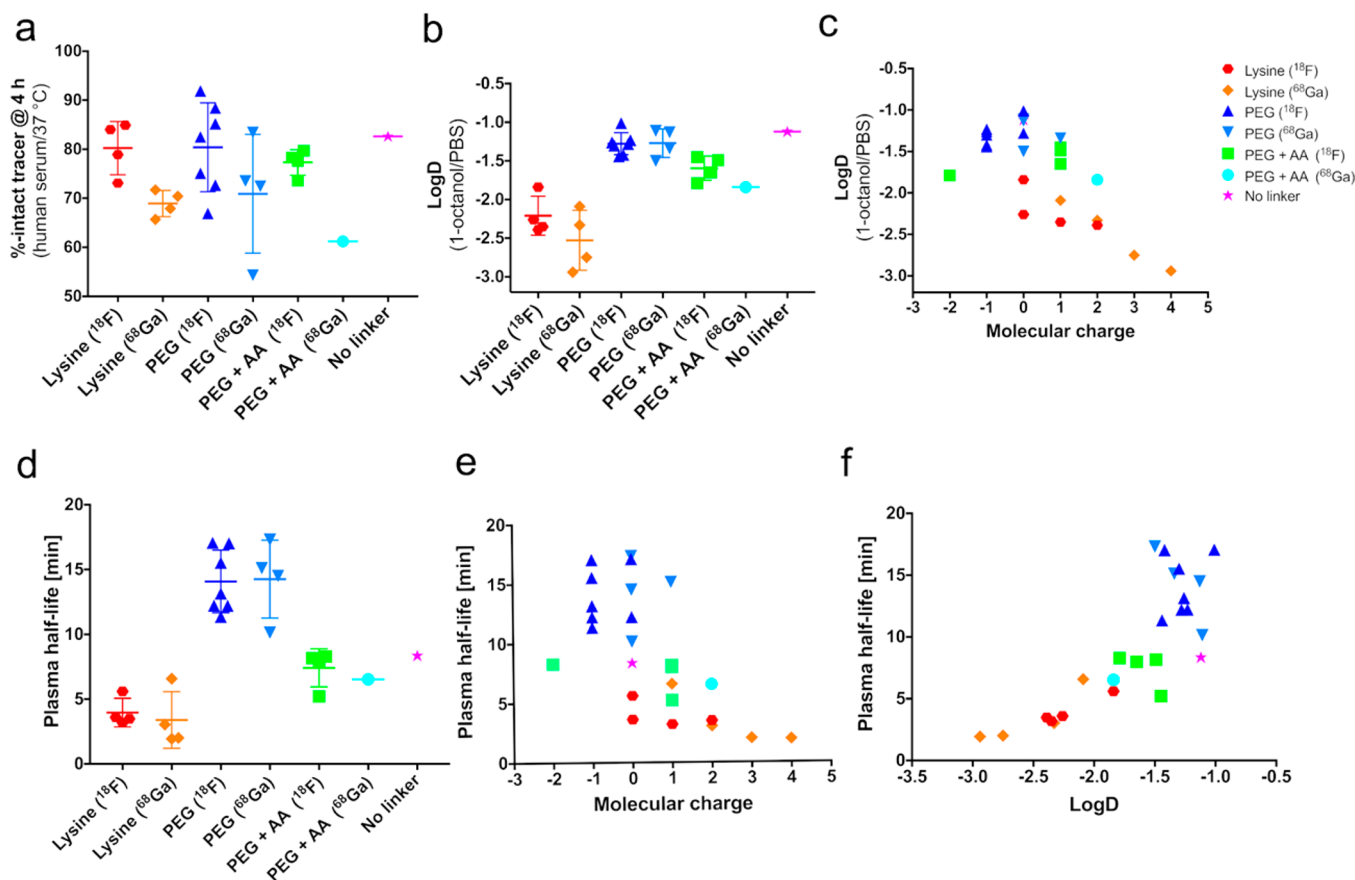


Figure 2. Correlation diagrams showing how structural and physicochemical parameters (e.g., stability, linker, molecular charge, log D , PHL) influence each other. (a) Tracer stabilities after a 3 h incubation time in human serum are shown after tracers were divided into groups with the same linker and radionuclide. Serum stabilities were generally >60%, except for ⁶⁸Ga-labeled compound **46**. (b) Log D values (median shown, $n = 3$) summarized as a group diagram. (c) Distribution coefficients in relation to molecular charge (under physiological conditions) showed a significant correlation. (d–f) in vivo PHLs plotted as a group diagram (d), in dependence of molecular net charge (e), as well as plotted against log D (f). Lysine-containing compounds showed overall fast clearance from circulation, with PEGylated compounds having three times longer PHLs. Interestingly, a positive correlation between a tracer's PHL and its log D value was found.

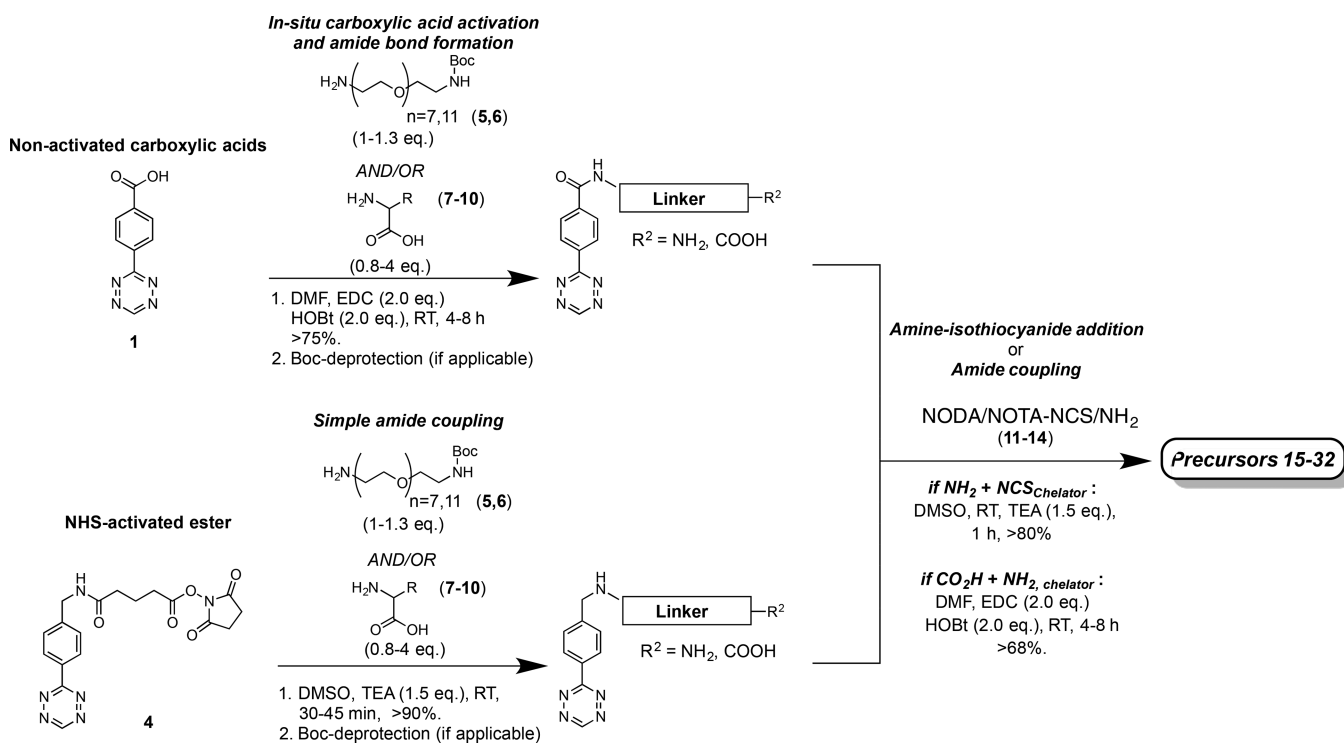
image-derived uptake data, justifying the use of image-derived organ uptake data for the majority of compounds in order to reduce the number of animals euthanized. Data analysis led to the selection of 15 radioligands (Table 1, highlighted in blue) that were further tested in in vivo pretargeting experiments using athymic nude mice bearing subcutaneous pancreatic ductal adenocarcinoma (PDAC) xenografts ($n = 4$). A TCO-modified immunoconjugate of the CA19.9-targeting antibody 5B1 (5B1–TCO; 1.3 nmol, 200 μ g per mouse) was injected 72 h prior to the injection of the small molecule radioligands (1.3–1.6 nmol, 0.6–1.4 μ g, 1–1.2 equiv). PET images were acquired hourly between 1–4 h p.i. unless stated otherwise. In addition, ex vivo biodistribution experiments were conducted for selected tracers in order to obtain quantitative information on tracer distribution in up to 14 organs. Ultimately, this investigation identified two radioligands ([¹⁸F]**27** and [⁶⁸Ga]**27**) as the most promising lead compounds (Table 1, highlighted in red).

Physicochemical and Pharmacokinetic Properties of Tz-Derived PET Tracer. Structural, in vitro, and pharmacokinetic (PK) data obtained for all 25 tracers were used to investigate potential correlations between physicochemical parameters. Tracer stabilities (given as % intact, $n = 3$) in human serum (incubation for 4 h at 37 °C, Figure 3c) ranged from >90% ([¹⁸F]**23**) to $54 \pm 7\%$ ([⁶⁸Ga]**24**) (Figure 3a, Supporting Information, section 4). Considering all of the structural

elements of the radioligands, we reasoned that both the tetrazine moiety and the metal complex would have an impact on in vitro (and presumably in vivo) stability. However, we found that instability was due primarily to the decomposition of the tetrazine moiety and that the radioactive metal complexes were stable over the course of our experiments. The majority of the radioligands did not show any elevated protein binding (<2% of total radioactivity, Supporting Information, section 4), with the exception of [¹⁸F]**20**, [¹⁸F]**21**, [⁶⁸Ga]**21**, [⁶⁸Ga]**22**, and [¹⁸F]**29**, each of which exhibited up to 16% protein-bound radioactivity. This result may be explained by the high lysine content residues and positive charge of these radioligands, prompting electrostatic interactions between the tracers and plasma proteins.²⁴

Not surprisingly, a significant negative correlation between the log D value of a tracer and its overall molecular charge under physiological conditions was found (p value <0.0001, Supporting Information, sections 4 and 9). Generally speaking, the closer the net charge of a tracer is to 0, the higher its partition coefficient. However, it is not quite that simple. For instance, radioligands possessing the same overall molecular charge but a different number of formally charged functional groups could still show significant differences in their distribution coefficients. One explanation could be enhanced solvation by water molecules through charge–dipole interactions: if the molecule exhibits a greater number of formal charges, it would lead to a higher

Scheme 1. Reaction Scheme Exemplifying the Synthesis of Precursor Molecules Using Tz 1 and Tz 4 via Two Different Synthetic Routes, Both of Which Furnish Final Compounds in Good Overall Yields and High Chemical Purities⁴



⁴For Tz starting materials such as Tz 1, in situ activation of the carboxylic acid group under mild conditions was performed using 1-ethyl-3-(3-dimethylamino-propyl)carbodiimide (EDC) and 1-hydroxybenzotriazole (HOBT), enabling subsequent amide coupling with the terminal amine of an appropriate linker moiety. NHS-activated, commercially available starting materials such as Tz 4 could be coupled to the linker moiety under weakly basic conditions with high conversion rates and without the need for further activation reagents. After TFA-mediated deprotection of the terminal Boc-group (if applicable), terminal amines (or carboxylic acids) were reacted with a bifunctional NODA or NOTA chelator construct that possessed a complementary functional group for chemical ligation.

degree of solvation.²⁸ For example, radioligands with a net charge of 0 containing a PEG linker (or no linker) exhibited log *D* values between -1.0 and -1.5, while radioligands with the same overall charge but with lysine residues in the linker displayed log *D* values between -1.8 and -3.1. PHLs for the radioligands correlated (*p* value <0.0001, Supporting Information, sections 5 and 9) with their net charge. Tracers with lower (more negative) log *D* values and higher net charges possessed shorter PHLs (Figure 3d,e). The replacement of a PEG linker by AAs or the incorporation of AA(s) to an already existing PEG linker resulted in reduced PHLs. PEG-containing tracers [¹⁸F]21-[⁶⁸Ga]28, even though ranging from -1 to +1 in terms of net charge, possessed calculated PHLs of >10 min. For instance, lead compounds [¹⁸F]27 and [⁶⁸Ga]27 exhibited PHL of 17.1 and 15.1 min, respectively. In contrast, AA-containing radioligands exhibited PHLs < 10 min. Tracers that solely contained lysine moieties as linkers displayed the shortest PHLs, values that decreased further as the number of lysine residues increased. For example, [⁶⁸Ga]22 (with a charge of +4 and 3 lysine residues) possessed a PHL of 1.9 min, the shortest of all tracers. Longitudinal PET imaging experiments conducted in healthy animals revealed a significant difference in biodistribution patterns and clearance pathways between tracers (Supporting Information, section 7). In general, lysine-containing radioligands (regardless of the presence of a PEG group) showed fast clearance from circulation and relatively high kidney radioactivity concentration of >5%ID/g as early as 1 h p.i. Radioactivity uptake and retention increased in a nearly linear fashion with the number of lysine residues per radioligand

(Figure 4a-c). High retention of the tracers containing lysine residues was likely due to reabsorption of those tracers in the proximal tubules of the kidney. In fact, recent studies have shown that peptides high in lysine residues are powerful kidney targeting agents, facilitating the uptake and retention of those constructs in the renal clearing organs.^{29,30} All other radioligands that did not contain lysine residues exhibited significantly lower kidney activity concentrations (<3.5%ID/g, Figure 4). Compound [⁶⁸Ga]30, for instance, exhibited the lowest uptake values of 1.2 ± 0.3%ID/g at 2 h p.i., although it also displayed higher liver (>1.8%ID/g) and intestinal uptake (>3%ID/g). Generally, tracers with overall net charges were cleared faster from circulation through globular filtration, whereas compounds with low or no net charge exhibited elongated circulation times and were predominantly cleared hepatically and excreted via the intestines.

Evaluation of Pretargeting Performance in a PDAC Xenograft Model. On the basis of this in vitro and PK data, 15 radioligands were selected for in vivo pretargeting experiments to probe correlations between PK parameters and pretargeting performance. Compounds were selected in order to cover a broad range of structural and physicochemical diversity. Generally, we reasoned that PHL and the primary clearance pathway of a tracer should have significant impact on its pretargeting performance. PHL would determine how much tracer molecules reach the target site before clearance, and the clearance pathway should influence the target-to-background ratio, as renal clearance should reduce background noise more quickly than hepatic clearance.

Explore Litigation Insights

Docket Alarm provides insights to develop a more informed litigation strategy and the peace of mind of knowing you're on top of things.

Real-Time Litigation Alerts



Keep your litigation team up-to-date with **real-time alerts** and advanced team management tools built for the enterprise, all while greatly reducing PACER spend.

Our comprehensive service means we can handle Federal, State, and Administrative courts across the country.

Advanced Docket Research



With over 230 million records, Docket Alarm's cloud-native docket research platform finds what other services can't. Coverage includes Federal, State, plus PTAB, TTAB, ITC and NLRB decisions, all in one place.

Identify arguments that have been successful in the past with full text, pinpoint searching. Link to case law cited within any court document via Fastcase.

Analytics At Your Fingertips



Learn what happened the last time a particular judge, opposing counsel or company faced cases similar to yours.

Advanced out-of-the-box PTAB and TTAB analytics are always at your fingertips.

API

Docket Alarm offers a powerful API (application programming interface) to developers that want to integrate case filings into their apps.

LAW FIRMS

Build custom dashboards for your attorneys and clients with live data direct from the court.

Automate many repetitive legal tasks like conflict checks, document management, and marketing.

FINANCIAL INSTITUTIONS

Litigation and bankruptcy checks for companies and debtors.

E-DISCOVERY AND LEGAL VENDORS

Sync your system to PACER to automate legal marketing.